Supporting Information for

Self-Optimising Continuous-Flow Hydrothermal Reactor for Nanoparticle Synthesis

Cameron Jackson[a], Karen Robertson[a], Vitaliy Sechenyh[a], Thomas W. Chamberlain[b], Richard A. Bourne[c], Edward Lester[a]

a. Advanced Materials Research Group, Faculty of Engineering, University of Nottingham, Nottingham NG7 2RD, United Kingdom.
b. Institute of Process Research and Development, School of Chemistry, School of Chemical and Process Engineering, University of Leeds, Leeds, United Kingdom
c. School of Chemical and Process Engineering, University of Leeds, Leeds LS2 9JT, United Kingdom

Table of Contents

1. Design of experiment (DoE) study

Table 1. Results of the DoE study

Exp. code	Temperature [°C]	Total flowrate [ml·min^{-1}]	Flow Ratio	Hydrodynamic diameter [nm]	PDI
1	340	30	0.330	43.3	0.25
2	360	30	0.330	56.3	0.21
3	380	30	0.330	83.7	0.10
4	340	35	0.330	45.3	0.55
5	360	35	0.330	34.6	0.49
6	380	35	0.330	73.8	0.25
7	340	25	0.330	41.3	0.23
8	360	25	0.330	56.9	0.21
9	380	25	0.330	90.2	0.11
10	340	30	0.415	42.9	0.53
11	360	30	0.415	38.6	0.31
12	380	30	0.415	71.7	0.22
13	340	35	0.415	43.0	0.52
14	360	35	0.415	43.1	0.21
15	380	35	0.415	88.5	0.25
16	340	25	0.415	62.1	0.62
17	360	25	0.415	36.7	0.41
18	380	25	0.415	70.7	0.23
19	340	30	0.500	101.7	0.46
20	360	30	0.500	63.7	0.60
21	380	30	0.500	49.4	0.28
22	340	35	0.500	93.9	0.50
23	360	35	0.500	51.2	0.66
24	380	35	0.500	81.8	0.30
25	340	25	0.500	87.6	0.53
26	360	25	0.500	50.7	0.59
27	380	25	0.500	56.9	0.24
28	360	30	0.415	34.4	0.30
29	360	35	0.415	33.8	0.40
30	360	35	0.415	33.9	0.39

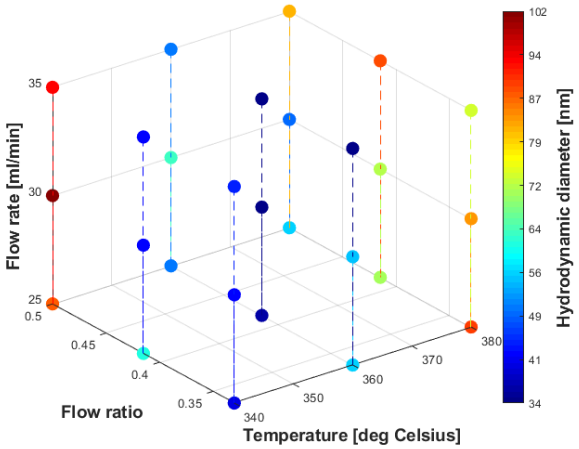

Figure 1. A plot showing outcomes of the DoE study. Each coloured point represents an individual experiment performed by the system.

2. Self-optimised experiments

Table 2. Results of self-optimised experiments using SNOBFIT optimisation algorithm

Exp. code	Temperature [°C]	Total flowrate [ml·min^{-1}]	Flow Ratio	Hydrodynamic diameter [nm]	PDI
1	372	27.2	0.361	62.1	0.22
2	372	26.9	0.373	64.3	0.21
3	360	30.0	0.330	56.3	0.21
4	361	27.5	0.346	57.2	0.23
5	380	26.3	0.347	75.9	0.18
6	368	27.9	0.396	51.0	0.23
7	364	26.7	0.330	68.8	0.24
8	360	25.0	0.330	58.2	0.20
9	380	29.2	0.330	83.7	0.14
10	369	28.1	0.354	59.3	0.22
11	366	27.7	0.347	57.6	0.20
12	378	29.3	0.396	60.5	0.20
13	380	26.0	0.330	81.9	0.18
14	376	27.6	0.359	64.0	0.21
15	368	32.1	0.377	44.6	0.23
16	380	25.0	0.338	77.8	0.16
17	374	31.5	0.383	51.9	0.17
18	373	25.0	0.346	60.7	0.17
19	380	25.0	0.330	91.1	0.13
20	364	25.5	0.335	72.8	0.25
21	380	27.7	0.358	76.0	0.21
22	365	33.5	0.345	42.7	0.31
23	378	28.4	0.330	75.8	0.21
24	377	25.0	0.330	77.7	0.23
25	376	26.9	0.343	73.9	0.23
26	377	27.3	0.346	74.5	0.22
27	380	28.2	0.354	74.5	0.21
28	380	26.2	0.330	84.1	0.17
29	380	29.3	0.330	78.7	0.19
30	380	25.0	0.330	84.4	0.18

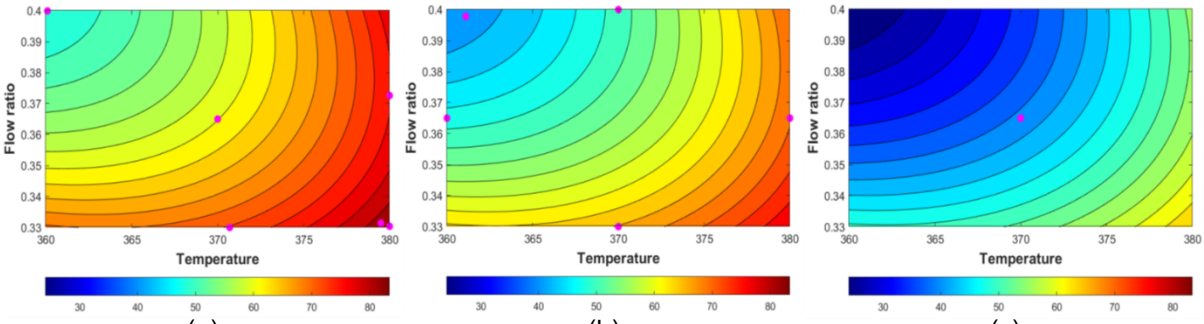

(a) (b) (c)

Figure 2. Contour plots of the polynomial regression model which was generated in self-optimised experiments using SNOBFIT algorithm. The pink dots show the position of individual experimental conditions. Plots correspond to following total flow rates: (a) – 25 ml·min^{-1}; (b) – 30 ml·min^{-1}; (c) – 35 ml·min^{-1}

Table 3. Results of self-optimised experiments using Bayesian optimisation algorithm

Exp. code	Temperature [°C]	Total flowrate [ml·min-1]	Flow Ratio	Hydrodynamic diameter [nm]	PDI
1	360	30.0	0.365	44.5	0.24
2	370	25.0	0.365	62.5	0.22
3	370	30.0	0.330	66.4	0.21
4	370	30.0	0.400	49.1	0.22
5	370	35.0	0.365	42.1	0.32
6	380	30.0	0.365	69.8	0.19
7	380	26.0	0.330	83.9	0.13
8	370	26.8	0.356	58.7	0.18
9	373	27.0	0.330	69.0	0.22
10	373	31.4	0.382	53.3	0.21
11	371	25.0	0.330	64.0	0.21
12	368	28.1	0.356	54.5	0.19
13	380	25.9	0.330	84.3	0.18
14	380	25.0	0.331	83.3	0.18
15	380	25.0	0.373	76.8	0.19
16	364	25.5	0.333	72.1	0.24
17	361	30.4	0.398	43.2	0.39
18	378	26.3	0.330	77.9	0.19
19	380	25.5	0.330	84.9	0.16
20	380	32.1	0.399	64.4	0.20
21	367	29.6	0.393	44.9	0.22
22	380	27.4	0.369	76.0	0.20
23	360	25.2	0.400	47.0	0.41
24	361	26.9	0.330	68.7	0.30
25	380	25.1	0.330	87.7	0.18
26	365	28.2	0.383	54.8	0.37
27	376	26.4	0.388	67.4	0.24
28	367	28.3	0.374	54.8	0.31
29	376	26.7	0.350	75.9	0.22
30	366	30.9	0.358	49.6	0.27

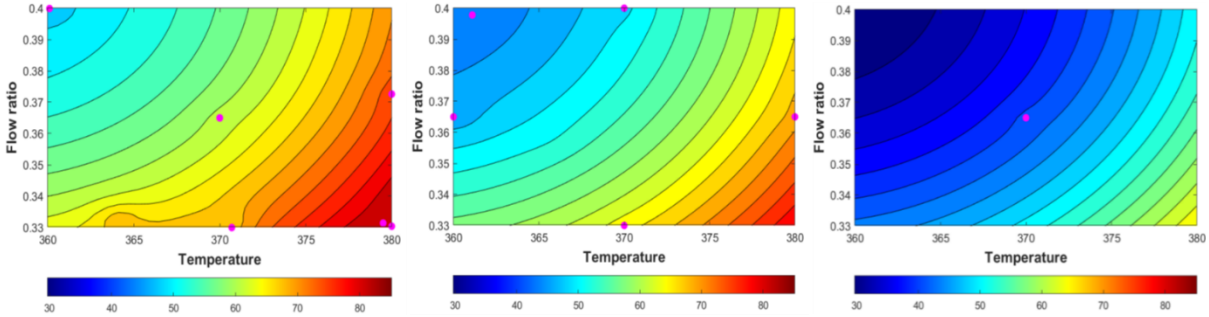

(a) (b) (c)

Figure 3. Contour plots of the Gaussian process regression model which was generated in self-optimised experiments using Bayesian optimisation algorithm. The pink dots show the position of individual experimental conditions. Plots correspond to following total flow rates: (a) – 25 ml·min^{-1}; (b) – 30 ml·min^{-1}; (c) – 35 ml·min^{-1}

3. Optimisation algorithm

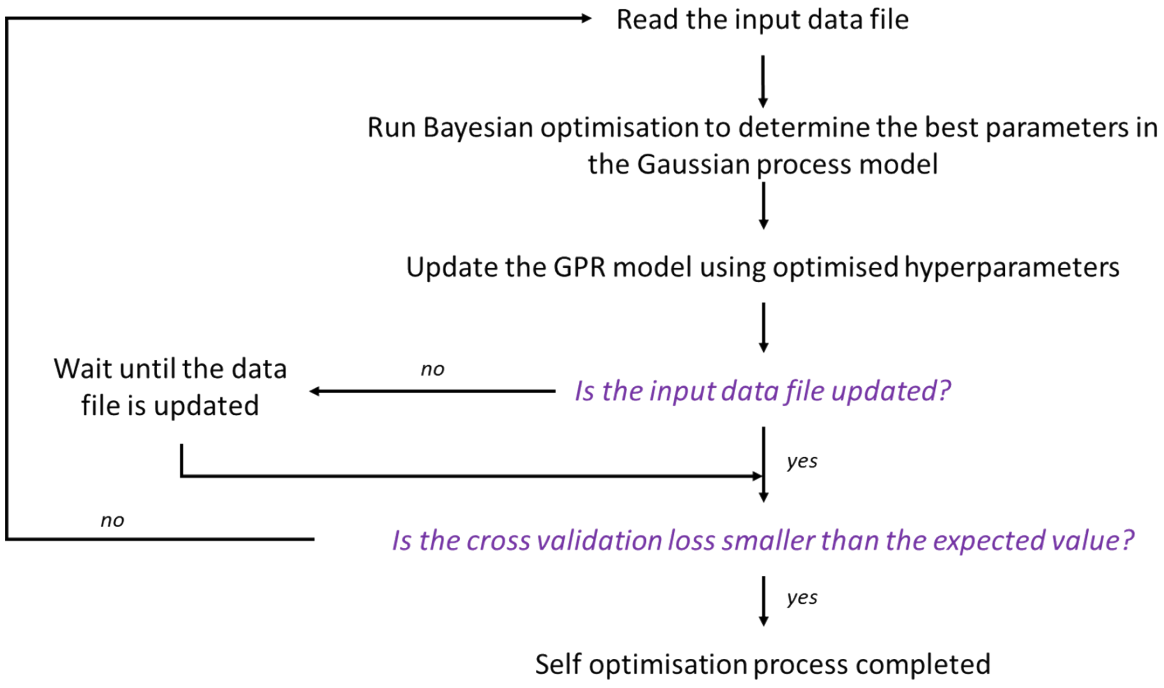

Figure 4. A simplified schematic of the algorithm used in self-optimised experiments.

4. DLS size distribution analysis

Count Rate (kcps):	360.0		**Measurement Position (mm):**	4.20
Cell Description:	Quartz flow cell		**Attenuator:**	6

		Size (d.nm):	**% Intensity:**	**St Dev (d.nm):**
Z-Average (d.nm): 45.41	**Peak 1:**	55.24	99.0	26.74
PdI: 0.195	**Peak 2:**	4495	1.0	879.4
Intercept: 0.941	**Peak 3:**	0.000	0.0	0.000
Result quality : Good				

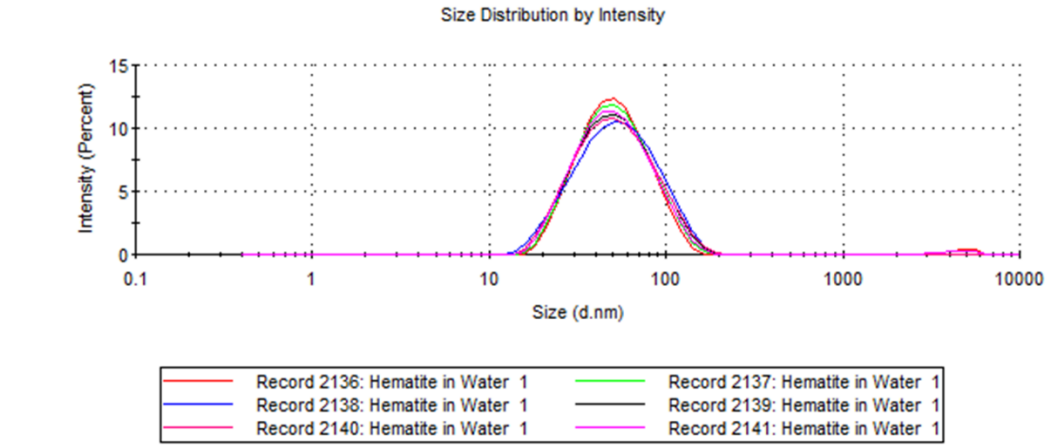

Figure 5. Results of the DLS analysis for Sample A. Plot includes information on the size distribution by intensity.

Count Rate (kcps):	420.8		**Measurement Position (mm):**	4.20
Cell Description:	Quartz flow cell		**Attenuator:**	6

		Size (d.nm):	**% Intensity:**	**St Dev (d.nm):**
Z-Average (d.nm): 54.08	**Peak 1:**	73.67	100.0	45.47
PdI: 0.225	**Peak 2:**	0.000	0.0	0.000
Intercept: 0.931	**Peak 3:**	0.000	0.0	0.000
Result quality : Good				

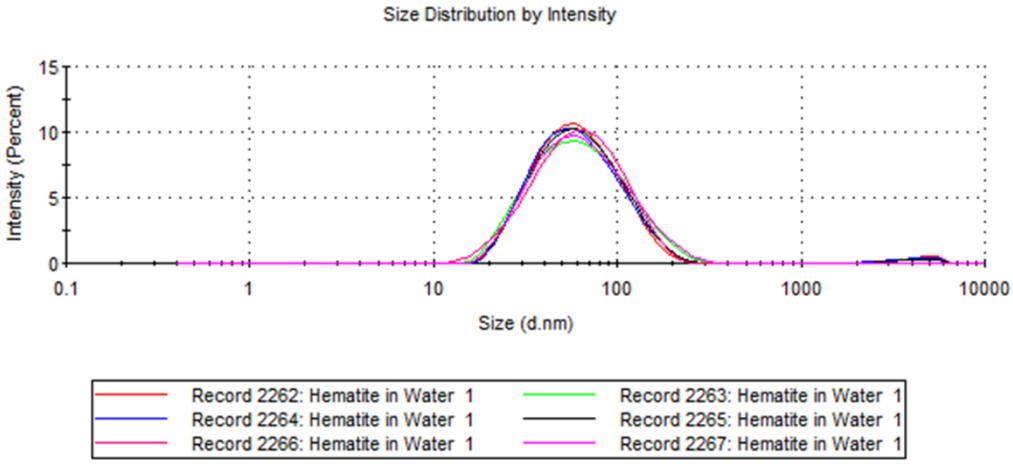

Figure 6. Results of the DLS analysis for Sample B. Plot includes information on the size distribution by intensity.

Count Rate (kcps):	301.4		**Measurement Position (mm):**	4.20
Cell Description:	Quartz flow cell		**Attenuator:**	5

			Size (d.nm):	**% Intensity:**	**St Dev (d.nm):**
Z-Average (d.nm):	66.95	**Peak 1:**	84.48	96.3	49.79
PdI:	0.252	**Peak 2:**	3503	3.7	1234
Intercept:	0.934	**Peak 3:**	0.000	0.0	0.000
Result quality :	Good				

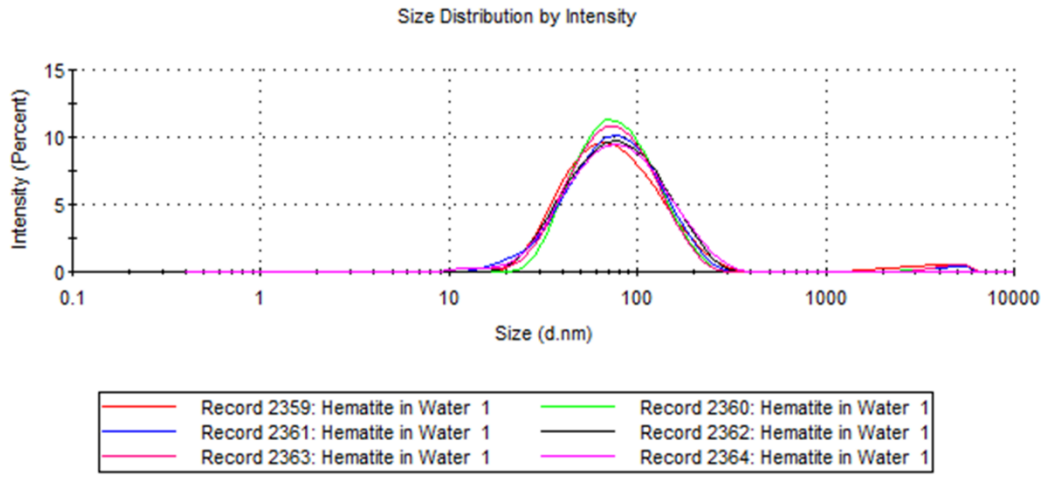

Figure 7. Results of the DLS analysis for Sample C. Plot includes information on the size distribution by intensity.

Count Rate (kcps):	301.6		**Measurement Position (mm):**	4.20
Cell Description:	Quartz flow cell		**Attenuator:**	4

			Size (d.nm):	**% Intensity:**	**St Dev (d.nm):**
Z-Average (d.nm):	76.17	**Peak 1:**	96.81	100.0	49.45
PdI:	0.214	**Peak 2:**	0.000	0.0	0.000
Intercept:	0.933	**Peak 3:**	0.000	0.0	0.000
Result quality :	Good				

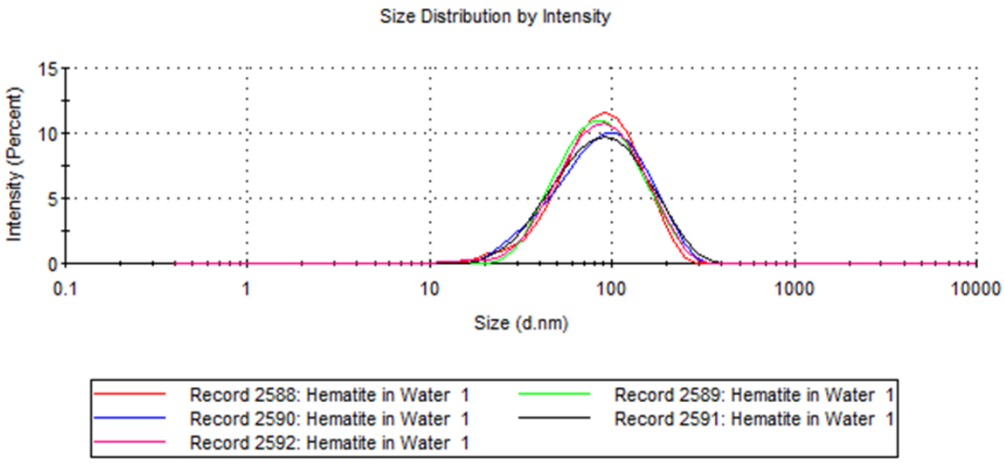

Figure 8. Results of the DLS analysis for Sample D. Plot includes information on the size distribution by intensity.

Count Rate (kcps):	362.6			**Measurement Position (mm):**	4.20
Cell Description:	Quartz flow cell			**Attenuator:**	4
			Size (d.nm):	**% Intensity:**	**St Dev (d.nm):**
Z-Average (d.nm):	84.05	**Peak 1:**	96.26	100.0	34.12
PdI:	0.131	**Peak 2:**	0.000	0.0	0.000
Intercept:	0.933	**Peak 3:**	0.000	0.0	0.000
Result quality :	Good				

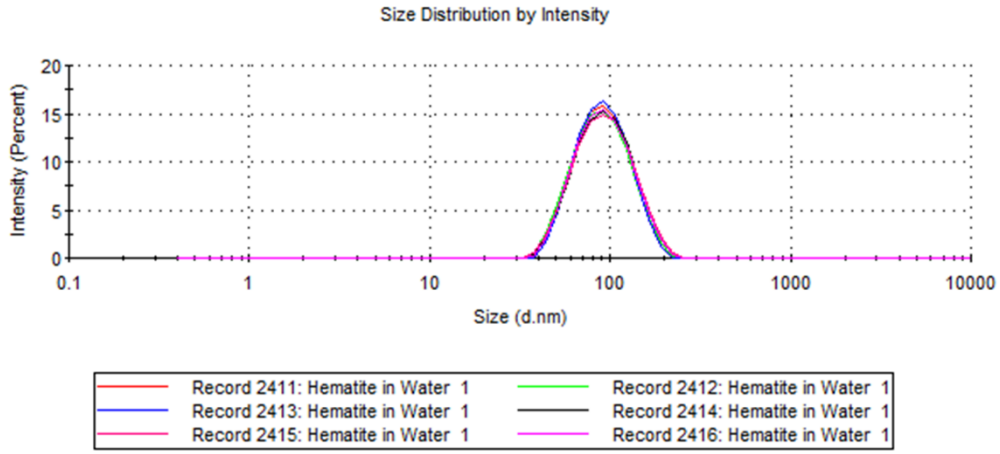

Figure 9. Results of the DLS analysis for Sample E. Plot includes information on the size distribution by intensity.

Count Rate (kcps):	272.0			**Measurement Position (mm):**	4.20
Cell Description:	Quartz flow cell			**Attenuator:**	4
			Size (d.nm):	**% Intensity:**	**St Dev (d.nm):**
Z-Average (d.nm):	91.71	**Peak 1:**	105.9	100.0	41.25
PdI:	0.122	**Peak 2:**	0.000	0.0	0.000
Intercept:	0.951	**Peak 3:**	0.000	0.0	0.000
Result quality :	Good				

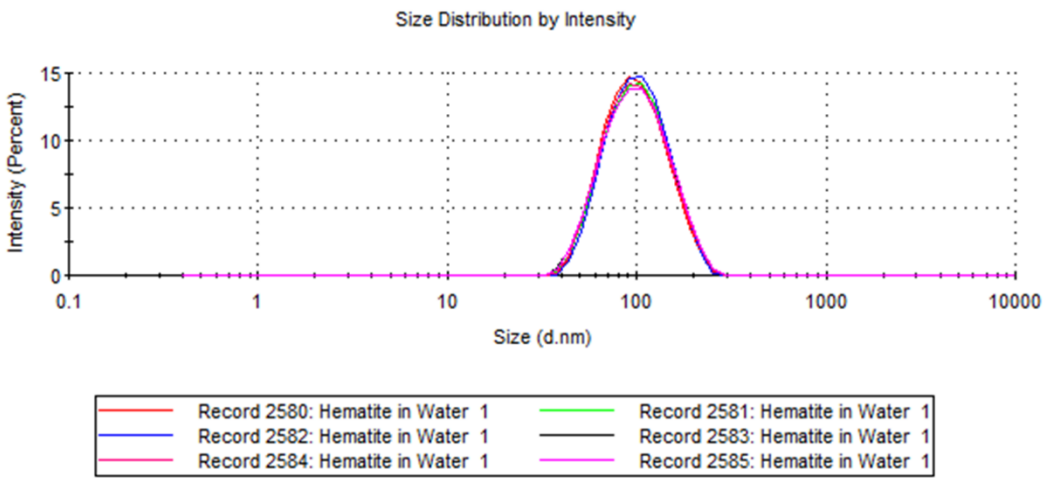

Figure 10. Results of the DLS analysis for Sample F. Plot includes information on the size distribution by intensity.

5. Validation of results using TEM, UV-vis and XRD techniques

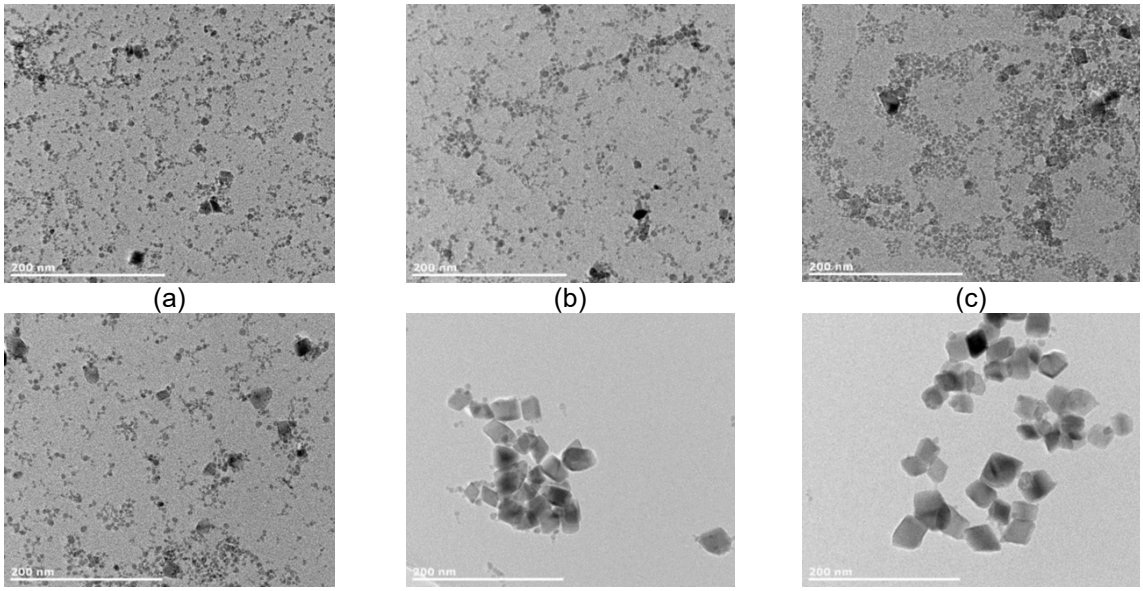

Figure 11. TEM images of following samples of nanoparticles: Sample A (a); Sample B (b); Sample C (c); Sample D (d); Sample E (e); Sample F (f).

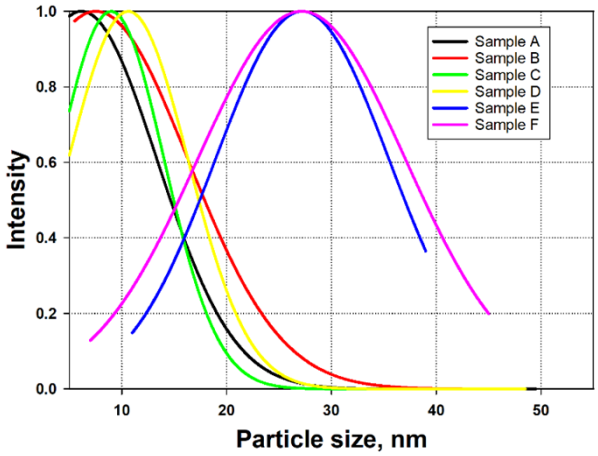

Figure 12. Comparison of particle size distributions obtained from TEM images of different samples

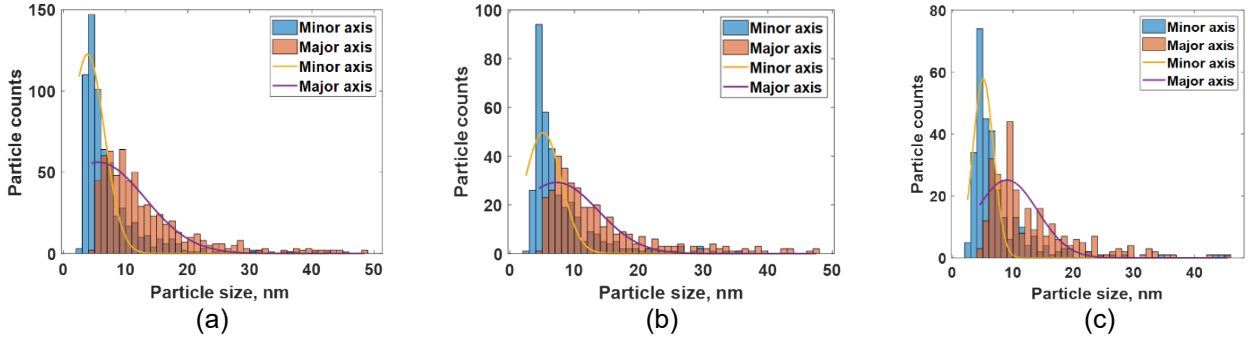

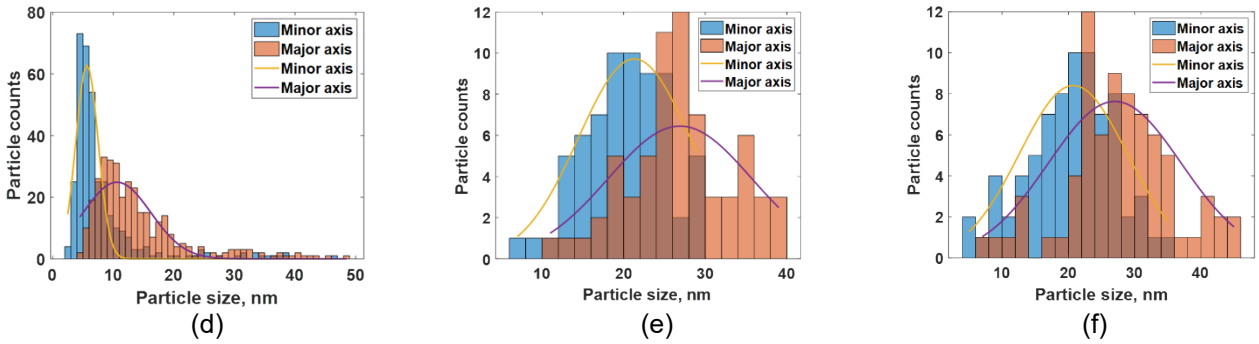

Figure 13. Particle size distributions for different samples of nanomaterials

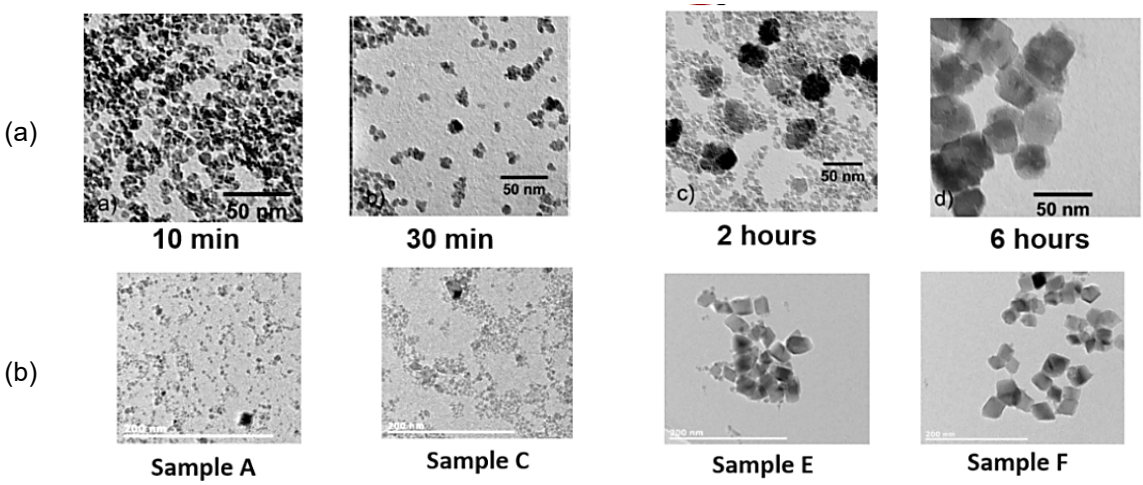

Figure 14. Comparison of TEM images obtained using two different types of nanomaterial synthesis: stirred tank reactor [1] (a); current study (b).

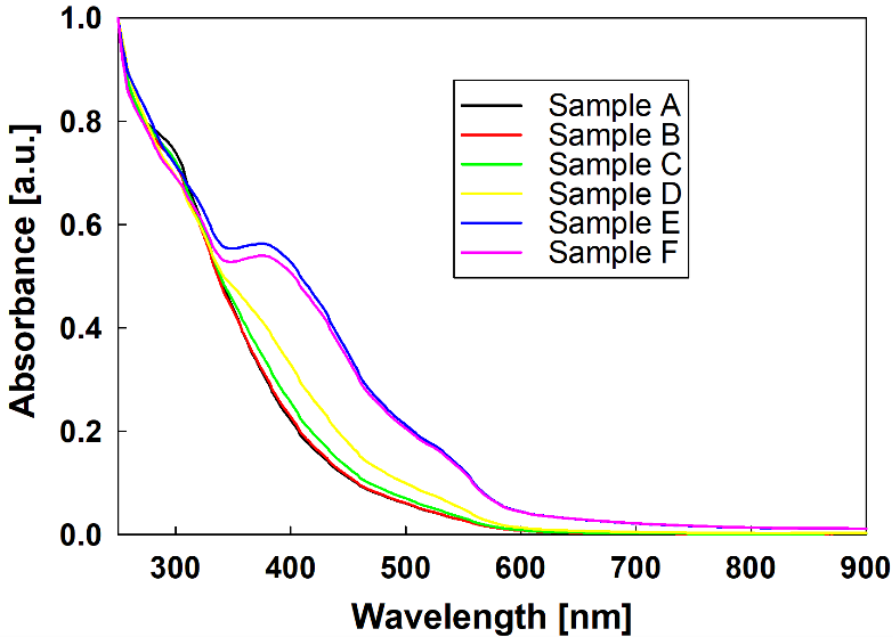

Figure 15. UV-Vis absorbance spectra of nanomaterial samples Cole-Parmer UV-Visible Spectrophotometer (WZ-83059-15) with a quartz cuvette of 10 mm path length. Analysis was in the wavelength range 250-900 nm, step size 2 nm.

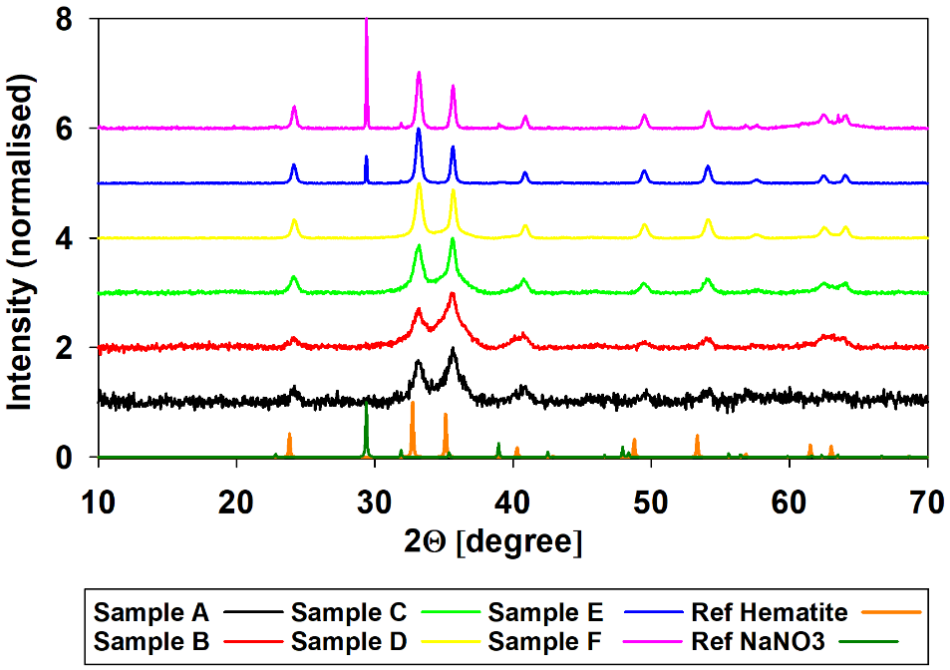

Figure 16. XRD spectra for different samples of nanomaterials Bruker D8-Advance Da Vinci Diffractometer with Cu Kα radiation (λ = 1.5418 Å). Diffraction patterns were recorded across a 2θ range of 5-70°, with a step size of 0.05° and 0.2 s per step

6. References

1 S. P. Schwaminger, R. Surya, S. Filser, A. Wimmer, F. Weigl, P. Fraga-García and S. Berensmeier, *Scientific Reports*, 2017, **7**, 12609.